



Porewater Carbonate Chemistry Dynamics in a Temperate and a Subtropical Seagrass System

Theodor Kindeberg^{1,2,3} · Nicholas R. Bates^{4,5} · Travis A. Courtney¹ · Tyler Cyronak^{1,7} · Alyssa Griffin¹ · Fred T. Mackenzie⁶ · May-Linn Paulsen¹ · Andreas J. Andersson¹

Received: 13 December 2018 / Accepted: 1 May 2020
© The Author(s) 2020

Abstract

Seagrass systems are integral components of both local and global carbon cycles and can substantially modify seawater biogeochemistry, which has ecological ramifications. However, the influence of seagrass on porewater biogeochemistry has not been fully described, and the exact role of this marine macrophyte and associated microbial communities in the modification of porewater chemistry remains equivocal. In the present study, carbonate chemistry in the water column and porewater was investigated over diel timescales in contrasting, tidally influenced seagrass systems in Southern California and Bermuda, including vegetated (*Zostera marina*) and unvegetated biomes (0–16 cm) in Mission Bay, San Diego, USA and a vegetated system (*Thalassia testudinum*) in Mangrove Bay, Ferry Reach, Bermuda. In Mission Bay, dissolved inorganic carbon (DIC) and total alkalinity (TA) exhibited strong increasing gradients with sediment depth. Vertical porewater profiles differed between the sites, with almost twice as high concentrations of DIC and TA observed in the vegetated compared to the unvegetated sediments. In Mangrove Bay, both the range and vertical profiles of porewater carbonate parameters such as DIC and TA were much lower and, in contrast to Mission Bay where no distinct temporal signal was observed, biogeochemical parameters followed the semi-diurnal tidal signal in the water column. The observed differences between the study sites most likely reflect a differential influence of biological (biomass, detritus and infauna) and physical processes (e.g., sediment permeability, residence time and mixing) on porewater carbonate chemistry in the different settings.

Keywords Carbonate chemistry · Carbon cycling · Estuarine processes · Blue carbon · Ocean acidification · Sediment · Early diagenesis · Interstitial water

Electronic supplementary material The online version of this article (<https://doi.org/10.1007/s10498-020-09378-8>) contains supplementary material, which is available to authorized users.

✉ Theodor Kindeberg
theo.kindeberg@gmail.com

Extended author information available on the last page of the article

1 Introduction

Coastal ecosystems play an important role in the global carbon cycle, largely due to the lateral transport of carbon and nutrients from rivers, terrestrial runoff and groundwater, intense benthic and pelagic metabolism and carbon transformation pathways in biomes such as seagrass beds, coral reefs, kelp forests, wetlands and saltmarshes (Duarte et al. 2005; Bauer et al. 2013). Seagrass beds are among the most productive marine ecosystems on Earth, trapping and storing a significant amount of carbon in their biomass and underlying soil (Duarte et al. 2005; Fourqurean et al. 2012; Mazarrasa et al. 2015). This makes seagrass an important contributor to what is known as blue carbon, or the ability of marine plants and ecosystems to help mitigate climate change by sequestering and storing anthropogenic CO₂ (Nellemann et al. 2009; Fourqurean et al. 2012; Mazarrasa et al. 2015; Howard et al. 2017). In addition to this important ecosystem service, seagrass beds also modify their surrounding seawater chemistry through the processes of photosynthesis and respiration. Several studies have proposed that seagrass beds are not only significant carbon sinks, but also provide a local buffering effect against ocean acidification (OA) and may act as refugia for marine species that are sensitive to lowered pH (Burdige and Zimmerman 2002; Barron et al. 2006; Semesi et al. 2009; Unsworth et al. 2012; Hendriks et al. 2014; Camp et al. 2016; Delgard et al. 2016; Cyronak et al. 2018a; Pacella et al. 2018).

Previous studies investigating the influence of seagrass on water column carbonate chemistry have predominantly focused on aboveground productivity whereas biogeochemical processes occurring in the underlying sediment have received far less attention (Delgard et al. 2016). Several studies have shown that porewater processes can play a significant part in modifying the overlying water column chemistry, which can be further amplified in the presence of seagrass (Burdige and Zimmerman 2002; Burdige et al. 2008; Deborde et al. 2008; Migné et al. 2016). For example, Burdige et al. (2002, 2008) showed that seagrass enhances carbonate sediment dissolution by fueling high rates of organic matter (OM) remineralization in the sediments by pumping oxygen via their roots and rhizomes that subsequently leads to elevated CO₂, lower carbonate saturation state (Ω) and elevated rates of carbonate mineral dissolution. These authors also proposed that the alkalinity generated from carbonate sediment dissolution in seagrass beds could constitute a negative feedback mechanism to increasing atmospheric CO₂ (Burdige and Zimmerman 2002; Burdige et al. 2008). Regardless of whether this is the case or not, the mechanism of transporting photosynthetically derived oxygen downward from shoots to roots (Smith et al. 1984; Caffrey and Kemp 1991; Borum et al. 2007) can have a significant influence on both porewater and water column chemistry. The release of oxygen into the sediments, known as radial oxygen loss (ROL), exerts a strong localized effect on the porewater chemistry surrounding the roots and rhizomes (Sand-Jensen et al. 1982; Borum et al. 2007). By inducing aerobic remineralization of OM, anaerobic redox processes are limited and reduced species are oxidized which lowers pH and consumes total alkalinity (TA) (Lee and Dunton 2000; Burdige and Zimmerman 2002; Brodersen et al. 2016). It is, however, not clear what the spatial extent of the oxygen release is and if it has implications for the biogeochemical processes farther than a few millimeters away from the roots (Greve et al. 2003; Ingemann Jensen et al. 2005; Frederiksen and Glud 2006; Brodersen et al. 2018). In addition to affecting oxygen levels, it has also been reported that seagrasses can utilize CO₂ from the porewater by transporting it to their shoots to sustain photosynthesis (Invers et al. 2001; Winkel and Borum 2009). Delgard et al. (2016) attributed this process to observations of net consumption of dissolved inorganic carbon (DIC) in porewaters underlying *Zostera noltii* beds

compared to adjacent unvegetated sediments which exhibited a net production of DIC. However, no measurement of diel variability in porewater DIC was carried out and it is therefore unknown to what extent this tentative process is modifying porewater carbonate chemistry (Delgard et al. 2016).

Regardless of the presence of vegetation, the relative production and consumption of DIC and TA in porewaters are largely governed by the early diagenetic processes in the sediment (Fig. 1; Krumins et al. 2013). Strong porewater gradients of DIC and TA are often observed in marine sediments, and concentrations typically increase with sediment depth as a result of aerobic and anaerobic mineralization processes (Mucci et al. 2000; Jourabchi et al. 2005; Rassmann et al. 2016).

However, it is not well known how porewater biogeochemistry changes over diel time scales and how local features such as tidal regime and sediment properties may interact with the presence of seagrass. Several studies from mangrove environments have reported tidally driven porewater fluxes which strongly influence the chemistry of overlying waters (e.g., Bouillon et al. 2007; Sippo et al. 2016; Tait et al. 2016; Taillardat et al. 2018). For instance, Taillardat et al. (2018) showed that a mangrove-dominated tidal creek was heavily influenced by porewater pumping during ebb tide, in which the mangrove porewaters contributed $46 \pm 14\%$ to increases in water column DIC. However, to the best of our knowledge, a complete characterization of diurnal variability of porewater carbonate chemistry in sediments colonized by seagrass has not been described in the literature.

Considering the role of coastal sediments and seagrass systems in marine biogeochemical cycles and dynamics, it is necessary to understand all parts of a seagrass ecosystem and

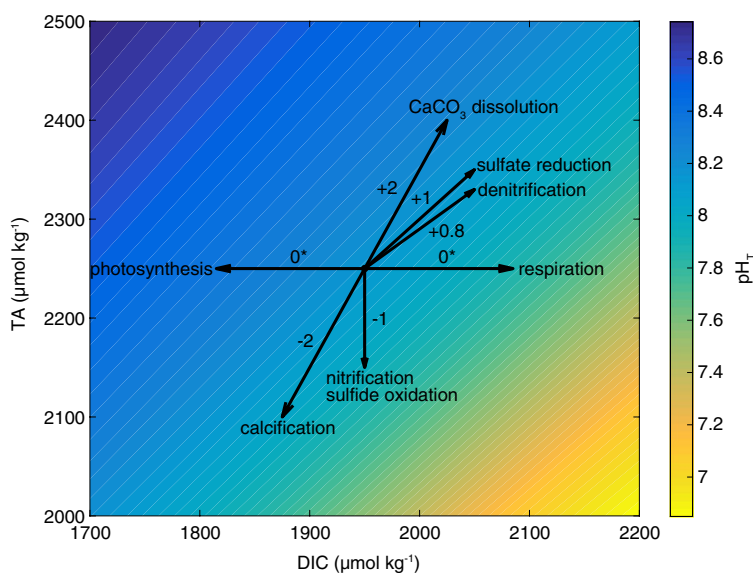


Fig. 1 Conceptual property-property plot of TA and DIC with pH_T isopleths. Arrows indicate sediment carbon chemistry and redox processes and their respective effect on DIC, TA and pH_T. Slopes (positive numbers) are based on the stoichiometry of equilibrium reactions from Krumins et al. (2013) (redox reactions) and Andersson et al. (2014) (carbonate chemistry reactions), while negative numbers represent the change in TA per mole O₂ consumed or mole CaCO₃ produced. The asterisk denotes that photosynthesis and respiration have a minor effect on TA (± 0.14 assuming Redfield stoichiometry). pH_T values are calculated using constant temperature (20 °C), salinity (34) and pressure (0 bar) and do not account for variation in redox conditions

its interplay with the surrounding environment. From an OA perspective, it is of particular interest to better understand how biogeochemical processes in the sediments modify carbonate chemistry in both the porewater and the overlying bottom water as this provides insights to the present-day conditions experienced by organisms (e.g., Rassmann et al. 2018). This includes improving our understanding and quantification of the role of seagrasses for sediment biogeochemistry, and constraining the physical, chemical and biological drivers of their spatial and temporal variability (Burdige 2006; Lessin et al. 2018; Middelburg 2018). The aim of this study was to elucidate the difference in carbonate chemistry parameters between the sediment porewater in contrasting seagrass environments in Mission Bay (San Diego, USA), representing a temperate, heavily modified estuary comprised of siliciclastic mud and a mangrove embayment in Mangrove Bay (Ferry Reach, Bermuda), representing a less altered, subtropical, carbonate sediment environment. At both locations, porewaters were sampled within the seagrass bed, while in Mission Bay samples were also taken from bare sediments without any aboveground seagrass vegetation. Our goal was to examine the following questions: (i) how do changes in porewater carbonate chemistry correlate with changes in the overlying water column?; (ii) is there a difference in vertical porewater profiles of DIC, TA and pH between the different study sites, including differences between the vegetated and unvegetated sediment in Mission Bay?; and, (iii) what is the diel variability of these parameters in the different sediments? These questions were addressed by conducting a 24-h study at each site measuring an array of physical and chemical parameters with temporal resolution ranging from minutes to hours.

2 Methods

2.1 Site Description

2.1.1 Mission Bay, San Diego

Mission Bay (32.79°–117.23°) is located in San Diego, California, USA (Fig. 2). It is a semi-enclosed but well-mixed, mesotidal estuary spanning 17.1 km² with extensive anthropogenic modifications including artificial islands and beaches (Obaza et al. 2015). Due to low freshwater inputs and high evaporation rates, Mission Bay is typically slightly hypersaline ($S \approx 34$ –36) compared to open ocean water (Largier et al. 1997). However, periods of heavy rainfall and freshwater discharge significantly lower the salinity of the bay (Elliott and Kaufmann 2007). Porewater salinity in Mission Bay has been found to range between 30 and 40 with an average (\pm SE) porewater salinity at the study site of 35 ± 1 (Talley et al. 2015). The Kendall-Frost Mission Bay Marsh Reserve is located in the north-eastern part of the bay, spanning approximately 65,000 m². The reserve is mainly comprised of a saltmarsh, mudflats, and, below the 0 m tide level, a vast eelgrass bed (*Zostera marina*) down to ~2 m depth (Levin 1984). The benthic community in the reserve consists mainly of dense patches of eelgrass with a few occurrences of widgeongrass (*Ruppia maritima*) (Johnson et al. 2003) growing on muddy, siliciclastic sediment. Shoot densities of *Z. marina* vary seasonally from as low as ~20 shoots m⁻² at temperature maxima in late summer and during storm events in the winter to > 300 shoots m⁻² in late fall and spring (Johnson et al. 2003). During the sampling period in Spring 2017, patches of dead *Z. marina* were observed, many of which were overgrown by ephemeral algae, as shown in the supplementary material (Online Resource 1).

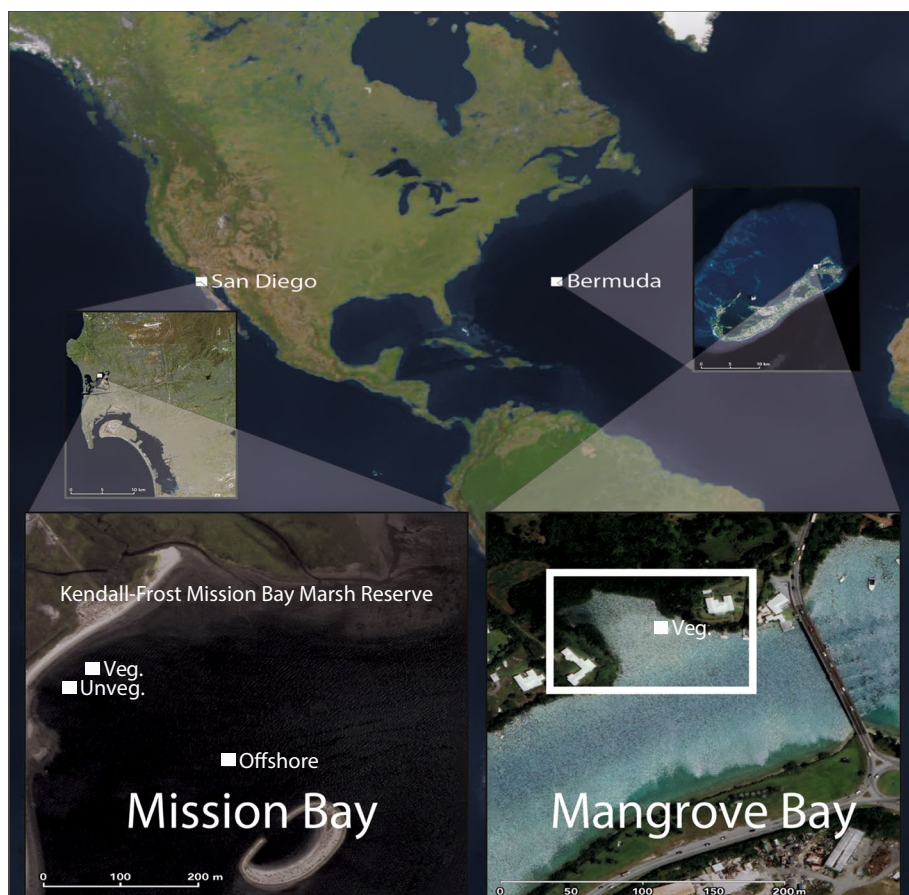


Fig. 2 Location of sampling sites in Mission Bay, San Diego, USA and Mangrove Bay, Ferry Reach, Bermuda. Shown are the sites of the porewater wells (vegetated and unvegetated) and where offshore reference samples were taken in Mission Bay. Mangrove Bay is denoted by a white rectangle

The weather was sunny and dry during the April 25–26, 2017 sampling event. However, the winter and early spring of 2017 (Jan–Apr) brought over 100 mm of precipitation to the area (<https://www.weather.gov/climate/index.php?wfo=sgx>).

2.1.2 Mangrove Bay, Ferry Reach, Bermuda

Mangrove Bay (32.37° –64.69°) is located on St. George's Island in the eastern part of Bermuda and is considerably smaller than Mission Bay, spanning approximately 3350 m² (Fig. 2). Freshwater input is supplied from rain- and groundwater (approximately 4% by volume), as no rivers or streams connect to the bay, and salinity has been found to range from 33.2 to 37.2 over a diel cycle (Zablocki et al. 2011). The benthic flora consists mainly of seagrass *Thalassia testudinum* and green algae surrounded by large stands of black and red mangrove trees (Zablocki et al. 2011). *T. testudinum* is prevalent but sparsely distributed across the bay with increased patchiness closer to shore. Shoot density has been found to range between 80 and 370 shoots m⁻² (unpublished data).

Sediments are comprised of carbonate mud with varying amounts of larger CaCO_3 grain sizes, mainly derived from calcareous algae and limestone (Lyons et al. 1980; Hines and Lyons 1982). Although at a similar latitude as San Diego, Bermuda's location in the North Atlantic Subtropical Gyre makes the climate subtropical with surface water temperatures ranging from 16 to 30 °C between winter and summer.

2.2 Sample Collection

2.2.1 Mission Bay, San Diego

A 24-h study was conducted in Kendall-Frost Mission Bay Marsh Reserve in Mission Bay, San Diego on April 25–26, 2017. During the entire study period (March–May), two temperature sensors (HOBO logger, Onset) recording temperature every 5 min were submerged in the sediment at 8 and 16 cm depth. Prior to the sampling study in April, two additional HOBO loggers measuring temperature and irradiance every 5 min were deployed on the bottom in the vegetated and unvegetated site. Illuminance data (in lux) were converted to photosynthetically active radiation (PAR) according to Long et al. (2012). Data of air temperature and precipitation were obtained from NOAA's National Climatic Data Center (NCDC, Menne et al. 2012).

Water column samples directly above the sediment–water interface (SWI) were collected immediately before and after each porewater well (PWW) sampling, using 250 mL Pyrex narrow-neck borosilicate glass bottles. Surface water samples ~500 m offshore from the PWW sites (Fig. 2) were collected immediately before PWW sampling to serve as a reference location. All water column samples were poisoned with 100 μL saturated solution of HgCl_2 and sealed according to standard protocol (Dickson et al. 2007). In conjunction with water column sampling, in situ temperature (± 0.3 °C), salinity ($\pm 1.0\%$) and dissolved oxygen (DO) ($\pm 2\%$) were measured with a YSI Pro2030 multiprobe (Xylem). Salinity was calibrated to seawater Certified Reference Material (CRM, Dr. A. Dickson, SIO) prior to sampling, and oxygen was calibrated in air at 100% humidity assuming 100% oxygen saturation.

Samples of sediment porewater were collected by submerging PWWs with intake at different depths in the sediment. All PWWs were constructed in the laboratory based on a modified design from Falter and Sansone (2000). PWWs were deployed in a dense patch of *Z. marina* covering depths of 2, 4, 6, 8, 12, and 16 cm below the SWI. PWWs were also deployed in an adjacent unvegetated area (~2 meters away) at the same depth and served as a control site. At each location, wells were deployed approximately 30 cm apart from each other to reduce the risk of overlapping with porewater extracted from adjacent wells (Falter and Sansone 2000; Drupp et al. 2016). All PWWs ($n=12$) were deployed four days prior to the sampling event. Porewater samples were collected four times during the 24-h study at morning high tide (HT), afternoon low tide (LT), evening HT and morning LT via freediving from a kayak (Table 1). Samples were collected using a 30-mL syringe that attached to the PWW 3-way stopcock valve through a luer lock connection. Depending on the depth of the PWW, a “dead” volume representing that of the entire tubing and well cylinder was first drawn and discarded in order to clear out water sitting in the well. Syringes with sample were taken back to shore and filtered through 0.45 μm Minisart® polyether-sulfone sterile filters (Sartorius) and placed in 25-mL glass vials. Filtering samples introduce a risk of CO_2 gas exchange which could influence DIC measurements. However, this procedure is necessary as extraction of porewater inevitably carries suspended colloidal

Table 1 Tides (relative to mean lower low water (MLLW)) in Mission Bay and relative water level height in Mangrove Bay during the sampling periods

Mission Bay		Mangrove Bay	
Time	Height (m)	Time	Height (m)
4/25/2017 09:12	1.55	9/18/2005 10:12	1.58
4/25/2017 15:23	0.03	9/18/2005 16:03	0.54
4/25/2017 21:17	1.89	9/18/2005 22:05	1.59
4/25/2017 04:07	-0.28	9/19/2005 03:57	0.56

Mission Bay (Crown Point) tide data were obtained from the National Oceanic and Atmospheric Administration (NOAA) Tides and Currents website (<https://tidesandcurrents.noaa.gov>). The tide in Mangrove Bay was measured every 2 h using a tidal stick. Water depth at morning low tide was ~30 cm at both sites

and clay-sized carbonate particles which would react with the acid addition in subsequent DIC and TA analyses. We employed a similar technique and same filter size as in Bockmon and Dickson (2014) in which no significant difference in DIC between filtered and unfiltered samples was observed. Samples were immediately poisoned with 25 μL HgCl_2 to cease any biological activity in the sample. Vials were sealed with a rubber stopper and an aluminum crimp seal. Concurrently, 5 mL of non-filtered and non-poisoned sample were used to measure pH using an Accumet glass electrode with an Orion Star Plus handheld pH meter (Thermo Scientific). The glass electrode was calibrated with a two-point calibration to NIST buffers (pH 4 and 7) and to tris(hydroxymethyl)aminomethane (Tris) buffer in artificial seawater (pH ~8.1 and salinity 35, prepared following recipe by DelValls and Dickson (1998)) to correct for the shift of the calibration curve due to salinity and to yield pH measurements on the total hydrogen ion scale (pH_T).

Sediment cores were collected three weeks after the sampling event using 30-cm-long transparent polycarbonate cylinders (Thermoplastic Processes) with an inner diameter of 7.3 cm. After the cylinder was emplaced into the sediment, a sealing lid was put on top of the cylinder to create a vacuum whereby a sediment core could be collected.

2.2.2 Mangrove Bay, Bermuda

A 24-h study was conducted between September 18–19, 2005 covering a full tidal cycle (Table 1). Water column ($n=13$) and porewater ($n=78$) samples were collected every 2 h between morning HT (10:12) and morning HT (10:03) the following day. However, due to issues with instrumentation, porewater samples of pH ($n=60$) were only collected until morning LT (03:57). Similar to the study in Mission Bay, temperatures were recorded in conjunction with each sampling using a temperature probe. Water column samples were collected using a 5 L Niskin sampler. Samples for DIC and TA were drawn into 200-mL Kimax glass bottles, poisoned with HgCl_2 and sealed for subsequent analysis at Bermuda Institute of Ocean Science (BIOS). Samples for DO were drawn into 115-mL BOD (Biological Oxygen Demand) bottles and immediately fixed with Winkler reagents. Samples for salinity were collected in salinity glass bottles. These DO and salinity samples were also analyzed at BIOS.

Porewater samples were collected in a sparse patch of *T. testudinum* in a similar manner to the Mission Bay study, using PWWs based on the same design and sampled at 2, 4, 6, 8, 12 and 16 cm below the SWI. For each porewater sample, a small volume was

drawn from the syringe into a small vial and analyzed for pH immediately after sampling. The remaining sample was then filtered, poisoned and transferred into sealed 25-mL glass vials for subsequent DIC analysis at BIOS. Surface and bottom water temperatures were recorded with a YSI in conjunction with each sampling (every 2 h). Two HOBO loggers were emplaced in the sediment at 8 and 16 cm depth, continuously recording temperature at five-minute intervals.

2.3 Sample Analysis

2.3.1 Mission Bay, San Diego

Porewater ($n=48$), bottom ($n=4$) and surface ($n=4$) water samples were analyzed for DIC, TA and pH in the Scripps Coastal and Open Ocean Biogeochemistry Laboratory at SIO. DIC was measured using an Automated Infrared Inorganic Carbon Analyzer (AIR-ICA, Marianda, Inc.) equipped with a LI-COR 7000 infrared CO₂ analyzer (Li-COR), with the average integrated value of a triplicate measurement (0.5 mL each) determined relative to the integrated value of a CRM (batch 149 and 151; Dr. A. Dickson, SIO). The average offset from the certified value was $-0.3 \pm 3 \mu\text{mol kg}^{-1}$. pH_T was determined spectrophotometrically using a Sami AFT-pH (Sunburst sensors, LLC) with meta-Cresol Purple (mCP) as indicator reagent. Accuracy and precision (-0.019 ± 0.008 units) of the instrument were periodically verified using either calculated pH_T of CRM (Dr. A. Dickson, SIO) or Tris buffer in artificial seawater (following recipe by DelValls and Dickson (1998)).

TA was determined using open-cell potentiometric titration with an 888 Titrand (Metrohm) titration system using an Ecotrode Plus pH glass electrode (Metrohm). Samples (10–15 g) were titrated with prepared 0.01 mol kg⁻¹ HCl in 0.6 mol kg⁻¹ NaCl and TA was calculated using a modified Gran function (Gran 1952). Accuracy and precision ($0.0 \pm 1.5 \mu\text{mol kg}^{-1}$) were determined using CRM. Measured values of TA were compared to calculated values (from DIC and pH_T) using the MATLAB program CO2SYS v. 1.1 (Lewis and Wallace 1998) with in situ values of temperature, salinity, DIC and pH_T as inputs. Dissociation constants K_1^* and K_2^* were adopted from Mehrbach et al. 1973 as refit by Lueker et al. (2000). TA samples with a mass below ~ 10 g ($n=17$) were diluted with de-ionized water (Milli-Q) prior to titration. A dilution factor was obtained by titrating multiple CRM samples ($n=8$) with different volumes of dilute in order to account for the nonlinear behavior of the electrode in diluted samples. A polynomial equation was parameterized to the offset from the certified CRM value and that equation was used to correct for the TA value of diluted samples. For samples that did not have sufficient volume for titration ($n=4$), the TA value calculated from DIC and pH_T as described above was used.

2.3.2 Mangrove Bay, Bermuda

Seawater samples were analyzed for DIC and TA following the same procedures described for Mission Bay samples, but with slightly different instrumentation. DIC was analyzed using an infrared analyzer (LI-COR 6262 NDIR) and TA was analyzed using a Brinkmann 665 Dosimat, equipped with a Brinkmann 654 pH meter (Metrohm) following the methods described in Dickson and Goyet (1994). Accuracy and precision for DIC and TA measurements were within $\pm 3 \mu\text{mol kg}^{-1}$ (CRM, batch 71). Samples for DO were analyzed by Winkler titration, following the procedures used by the Bermuda Atlantic Time-series Study (BATS) (Knap et al. 1997) and salinity was measured with an Autosol 8400A

salinometer (Guildline Instruments). Porewater samples were analyzed for DIC as previously described, and pH was determined immediately after sample collection using a hand-held Accumet AP72 glass electrode (Thermo Fisher Scientific), calibrated to NIST buffers. Note that calibration was only made with low ionic strength buffers, and thus, relatively high uncertainty is anticipated with respect to the absolute values of these measurements. However, comparison of calculated pH_T from DIC and TA of bottom water ($n=13$) with measured pH revealed an offset of 0.01 ± 0.003 pH units.

2.3.3 Sediment Analyses

Sediment cores ($n=2$) collected at the two sites in Mission Bay were photographed immediately after collection and brought back to SIO for subsequent grain size analyses. A plunger was used to extract the core from the sampler, the core was sliced into 2-cm-thick slices, and each slice was then cut in half. A subsample representative of the entire depth of each core was sieved through 1000, 500, 250, 125 and 63 μm mesh sizes. Particles smaller than 63 μm were collected in a separate container of deionized water and left for one week to settle. The different grain size fractions were dried in an oven at 60 °C for one week and weighed individually in order to calculate a relative mass (% dry weight) of bulk weight for each grain size.

In Mangrove Bay, no sediments were collected at the time of the study. However, a similar study took place in 2009 (unpublished data) when sediment samples from five different locations in the bay were collected. An average of grain size distributions from these five locations was used in the present study.

2.4 Data Analyses and Uncertainty Assessments

To evaluate the coupling between bottom water and porewater, the time lag between changes in temperature at different sediment depths was evaluated. The temperature lag within the sediment was defined as the time it takes for an observed temperature signal to propagate between two depths (0–8 cm, 8–16 cm and 0–16 cm, respectively) and was calculated by cross-correlation using the MATLAB function `xcorr`.

Grain size distributions were assessed using the Excel package GRADISTAT v.4.0 (Blott and Pye 2001). Differences in grain size distribution between the sites were assessed using a two-sample Kolmogorov–Smirnov test.

To assess relationships between TA and DIC, type II linear regressions were performed using the MATLAB script `lsqfitma.m` (<http://www.mbari.org/staff/etp3/regress.htm>), plotted on pH_T isopleths calculated with CO2SYS. Confidence intervals (CI 95%) of the slopes were used to assess difference in slopes between sites. Furthermore, to assess differences in average porewater concentrations of DIC and TA, the depth-integrated concentration was calculated as the sum of the concentrations at each depth multiplied by the respective depth interval (2 or 4 cm) and divided by the total sample depth (16 cm). The mean depth-integrated concentration of each sampling was calculated to obtain a diel average.

In order to calculate all parameters of the aqueous CO_2 system, two of the four master variables DIC, TA, pH or pCO_2 (partial pressure of CO_2) are needed in conjunction with temperature, salinity and pressure (Zeebe and Wolf-Gladrow 2001). In the Mission Bay study however, three master variables (DIC, TA and pH) were measured and pH was measured twice for each sample—both in conjunction with sampling using a glass electrode and subsequently in the laboratory by spectrophotometry. Over-determining the

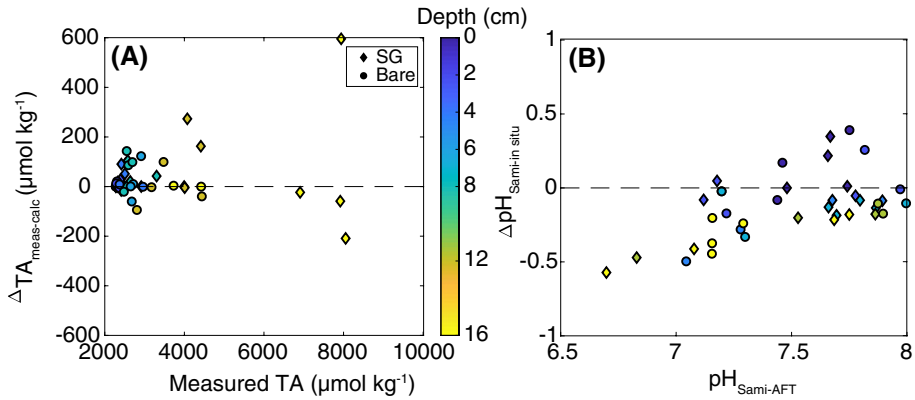


Fig. 3 **a** The difference between measured and calculated TA plotted against the measured TA ($n=51$). **b** The difference between pH_T measured in situ and pH_T measured with Sami AFT-pH ($n=38$). Colors indicate the sediment depth from which samples were collected

CO_2 system allows for additional quality control and assessment of potential errors and uncertainty. For example, measured (TA_{meas}) and calculated (TA_{calc}) values of TA (from DIC and pH_T) exhibited better agreement at shallower sediment depth, but the variability increased with sediment depth (Fig. 3a). In nearly all samples from ≥ 8 cm depth, HgS precipitated when HgCl_2 was added. This reaction reduces alkalinity and increases the uncertainty of the measurements (Goyet et al. 1991). Regrettably, precipitation of HgS was not quantified and its effect on TA is therefore not known, which constitutes a risk of underestimating TA and TA:DIC ratios at sediment depths ≥ 8 cm. TA_{meas} values were used in the results except where the sample volume was insufficient for titration and TA_{calc} was used instead ($n=4$).

When comparing pH_T values measured with glass electrode in situ to those measured spectrophotometrically in the laboratory, a pattern similar to that seen between calculated and measured TA was observed. In general, the pH_T values agreed well at shallower depths but the discrepancy increased with lower pH_T values (i.e., deeper depths) (Fig. 3b). Oxygen contamination and subsequent sulfide oxidation, HgS precipitation or a combination of the two could partly explain this discrepancy.

The seawater saturation state of CaCO_3 with respect to aragonite (Ω_{Ar}) was calculated using DIC and TA as master variables, with in situ temperature, salinity and pressure. Dissociation constants K_1^* and K_2^* were adopted from Mehrbach et al. 1973 as refit by Lueker et al. (2000).

3 Results

3.1 Water Column Variability of Environmental and Chemical Parameters

3.1.1 Mission Bay, San Diego

The tidal range in Mission Bay was 2.17 m with low tides at 15:23 and 04:07 and high tides at 9:12 and 21:17 during the study (Table 1). Water column temperature increased

during outgoing tides and decreased with incoming tides regardless of the time of day (Fig. 4). Hence, the warmest temperatures coincided with low tides and coldest temperatures with high tides. Longer-term recordings (April–May) of water column temperature in Mission Bay showed similar variability, largely controlled by the semi-diurnal tidal cycle (Online Resource 2). Salinity did not reveal any temporal trend (Fig. 4).

DIC and TA exhibited temporal variability that revealed combined influences from the light and tidal cycle with lower concentrations in the afternoon and evening, and higher in the mornings (Fig. 4). The highest DIC and TA values were observed at morning low tide and the lowest at evening high tide. pH_T and Ω_{Ar} exhibited the opposite trend with minimum values observed at morning low tide and maximum values observed at evening high tide (Fig. 4). Notably, the low DIC and TA and high pH_T and Ω_{Ar} values were observed in the evening after sunset and coincided with a relatively elevated, high tide. DO also showed a similar trend with lowest values in the morning and highest values during the evening high tide (Fig. 4).

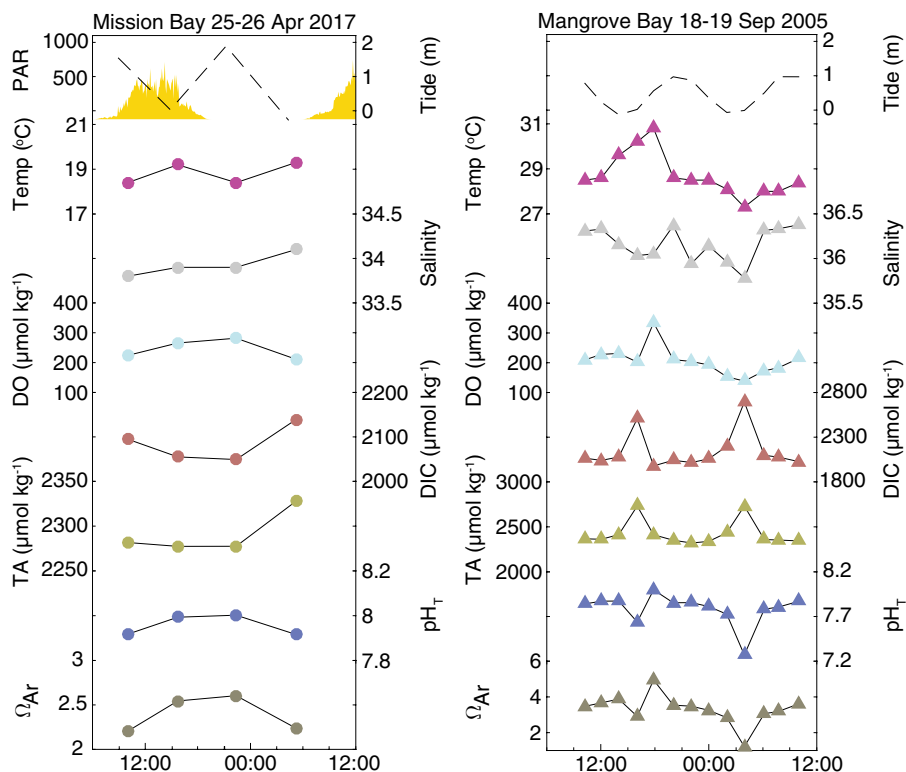


Fig. 4 Water column time series in Mission Bay (a) and Mangrove Bay (b) of tide, temperature, salinity, DO, DIC, TA, pH_T and Ω_{Ar} . In (a), photosynthetically active radiation (PAR) is also plotted, given in $\mu\text{mol m}^{-2} \text{s}^{-1}$

3.1.2 Mangrove Bay, Bermuda

Low and high tides in the Mangrove Bay study occurred at similar times as in the Mission Bay study (Fig. 4), but the 1 m tidal range was approximately half the range of Mission Bay tides (Table 1). Water column temperature reached a maximum of 30.8 °C in the late afternoon and a minimum of 27.3 °C at night coincident with low tide. Similar to Mission Bay, there was no clear trend in salinity albeit the lowest salinity value occurred at low tide at night (Fig. 4). Seawater carbonate chemistry properties strongly followed the tidal signal with maximum DIC and TA and minimum pH_T and Ω_{Ar} observed coincident with low tides regardless of the time of the day (Fig. 4). For all water column biogeochemical parameters, the largest change measured between two consecutive samplings occurred between slack water at low tide and the following sampling during flood tide. Between low tides, carbonate chemistry properties were relatively invariable. For most of the times, DO appeared to mirror DIC and tracked the trends in pH_T and Ω_{Ar} (Fig. 4).

3.2 Connectivity Between Water Column and Porewater Properties

Based on temperature measurements in the water column and within the sediments in both Mission Bay and Mangrove Bay, it appears that changes in the water column were translated into the sediment porewaters albeit with a time lag and dampened variability as one moves into the sediments (Fig. 5). That is, a decrease or increase in temperature in the water column was followed by a decrease or increase in porewater temperatures. Both the time lag and the dampening of variability increased with increasing sediment depth. In Mission Bay, the time lag was 2.4 h between 0 and 8 cm, 2.6 h between 8 and

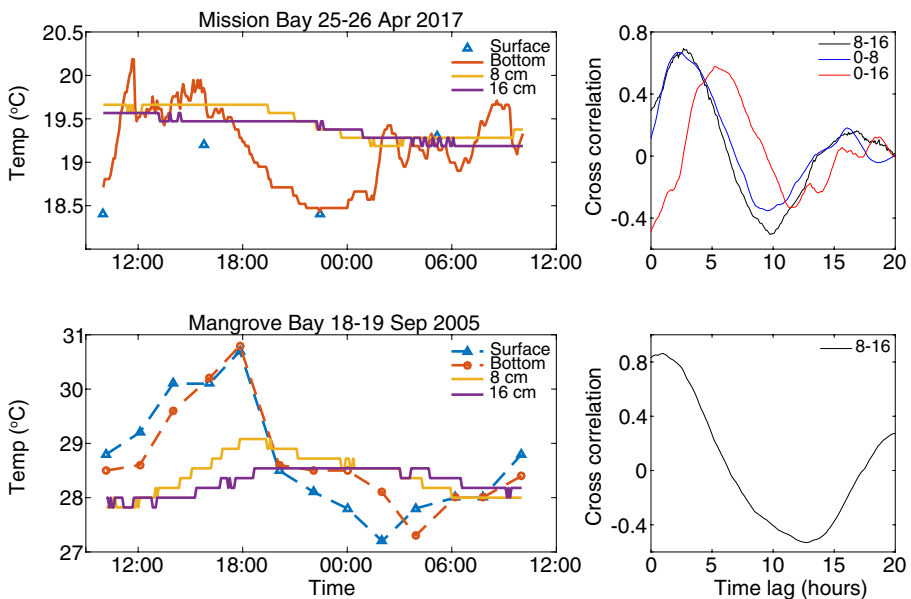


Fig. 5 Water column and porewater temperatures at 8 and 16 cm in Mission Bay (a) and Mangrove Bay (b). c and d show the time lag in temperature between the different depths. This was obtained by cross-correlation where the dominating lag time is illustrated by the first peak of respective depth interval

16 cm and 5 h between 0 and 16 cm (Fig. 5). Similar lags and dampening of variability were observed in Mangrove Bay, but the observed time lag between porewater temperatures at 8 and 16 cm was < 1 h. Longer-term monitoring (April–May) of temperature in the bottom waters and in sediments of Mission Bay reaffirmed that the observed correlation and lag between bottom water and porewater were temporally consistent properties at this site (Online Resource 2). No such long-term observations were available for Mangrove Bay.

3.3 Porewater Carbonate Chemistry Properties and Variability

Overall, the mean and the temporal variability in porewater carbonate chemistry parameters differed between the different locations and exhibited marked vertical zonation through the sediment. In general, DIC and TA increased and pH_T and Ω_{Ar} decreased with sediment depth (0–16 cm). Over the 24-h studies, Mission Bay and Mangrove Bay differed in that a semi-diurnal signal in porewater chemistry was observed at some depths in Mangrove Bay whereas no pronounced temporal trend was observed in Mission Bay (Figs. 6, 7).

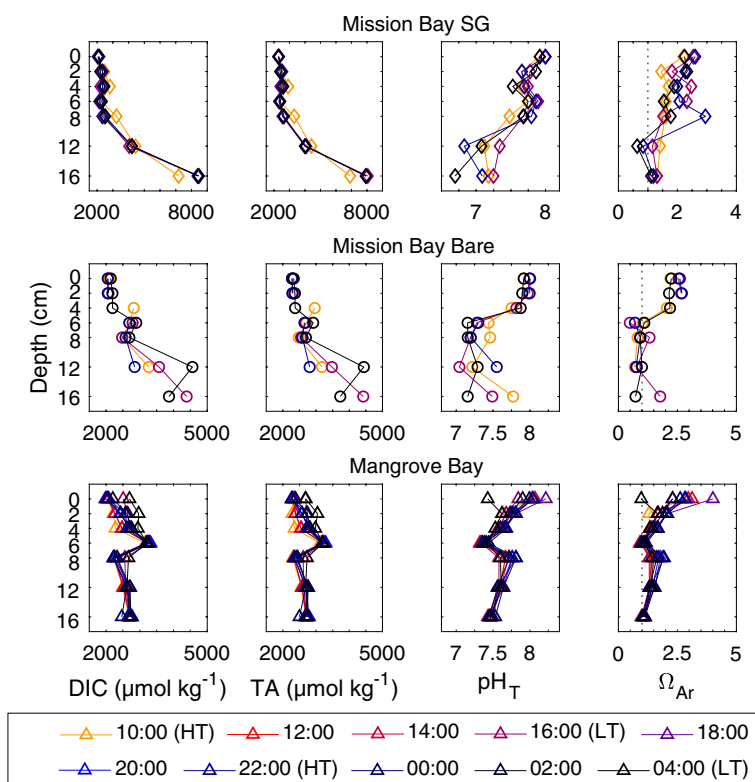


Fig. 6 Vertical porewater profiles of DIC, TA, pH_T , and Ω_{Ar} for Mission Bay Seagrass ($n=28$) (top panel), Mission Bay Bare ($n=23$) (mid panel) and Mangrove Bay Seagrass ($n=70$) (bottom panel). Dashed line in Ω_{Ar} plots indicate $\Omega_{Ar} = 1$. Note that x-axis limits differ between sites

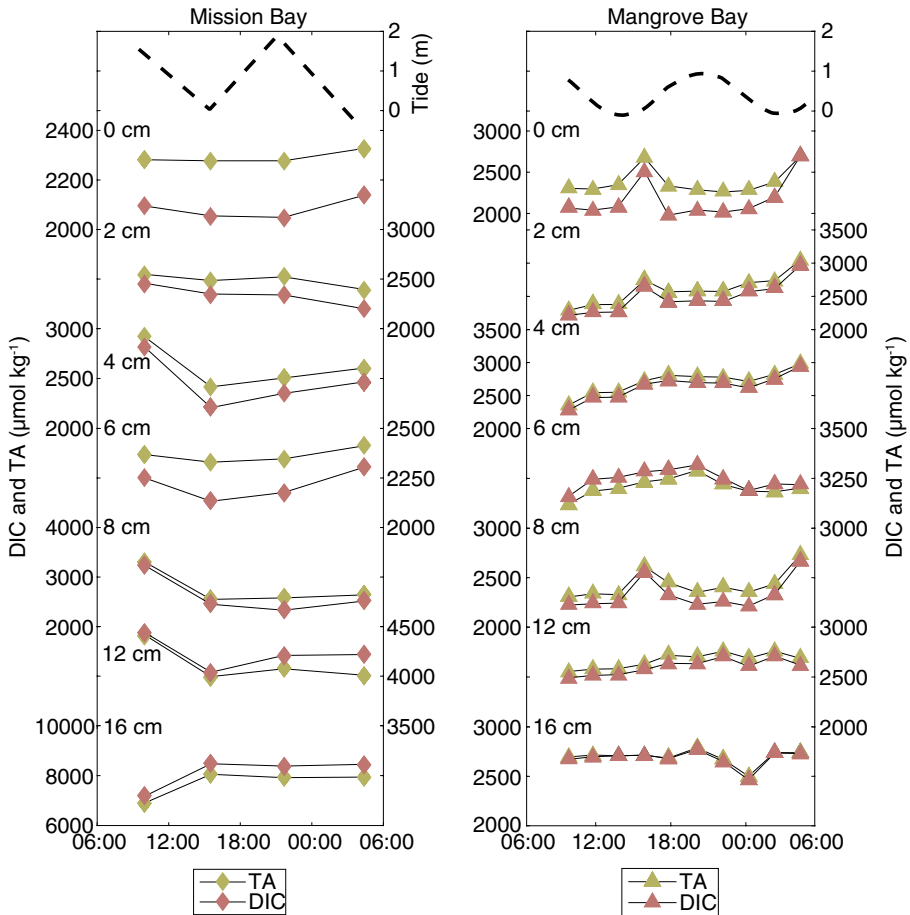


Fig. 7 Time series of porewater DIC and TA at different sediment depths for Mission Bay (left) and Mangrove Bay (right). Only the seagrass site in Mission Bay is shown

3.3.1 Vertical Distribution and Variability

3.3.1.1 Mission Bay, San Diego The vertical porewater profiles of carbonate parameters exhibited strong gradients at both the vegetated and unvegetated sites with increasing concentrations of DIC and TA with sediment depth. These parameters were relatively constant from the SWI down to 8 cm where a large increase down to 16 cm was observed. At the seagrass site, the diel depth-integrated (0–16 cm) DIC and TA were on average 4293 ± 45 and $4489 \pm 506 \mu\text{mol kg}^{-1}$, respectively. The vertical variability was largest at the Mission Bay seagrass site with average DIC and TA values increasing more than threefold between 8 and 16 cm (Fig. 6). Similar patterns were observed for pH_T and Ω_{Ar} , and the porewater at 12 cm was undersaturated with respect to aragonite during evening HT and morning LT (Fig. 6).

At the unvegetated Mission Bay site, porewater profiles of carbonate parameters were different compared to the seagrass site, albeit with maxima and minima at the same depths. Average DIC and TA values were generally lower than in the seagrass sediment, with a depth-integrated diel average of 3066 ± 304 and $3060 \pm 298 \mu\text{mol kg}^{-1}$, respectively. The

largest difference was observed at 16 cm where the concentrations of DIC and TA were about half as high as in the seagrass sediment. A similar trend was observed in pH_T where a distinct drop of ~ 0.5 pH_T units was seen between 4 and 6 cm depth. Porewaters in the unvegetated site were consistently undersaturated with respect to aragonite at 12 cm depth and, during all but the afternoon sampling, at 8 cm depth (Fig. 6).

3.3.1.2 Mangrove Bay, Bermuda Porewater vertical profiles of carbonate parameters showed markedly different patterns in Mangrove Bay compared to Mission Bay. Overall, the range between minimum and maximum concentrations of porewater carbonate parameters across depth was considerably lower than that observed in Mission Bay and the profiles exhibited a much different shape (Fig. 6). Here, values of DIC and TA increased with depth down to a distinct inflection point at 6 cm depth. Beyond this depth, DIC and TA decreased down to 8 cm depth and then gradually increased with depth to 16 cm depth. Average depth-integrated DIC and TA over the study period was 2657 ± 86 and 2708 ± 83 $\mu\text{mol kg}^{-1}$, respectively. The vertical profiles of pH_T and Ω_{Ar} exhibited a similar inflection point with lowest values observed at 6 cm. At this depth, porewaters were undersaturated with respect to aragonite 60% of the time (Fig. 6).

3.3.2 Temporal Variability

3.3.2.1 Mission Bay, San Diego No apparent temporal trends in porewater carbonate parameters were observed at either site in Mission Bay. At the seagrass site, concentrations of DIC and TA co-varied and exhibited the largest temporal variability in absolute concentrations at 8 and 16 cm whereas the largest relative change between two consecutive samplings occurred at 4 and 8 cm between morning HT and afternoon LT (Fig. 7). The temporal variability of pH_T varied greatly between depths ranging from 7.25 to 6.70 at 16 cm and from 7.89 to 7.75 at 6 cm, between afternoon LT and morning LT (Fig. 6).

At the unvegetated site, fewer samples were collected ($n=19$) due to some of the PWWs periodically clogging which made it difficult to interpret temporal variability for porewater at 4 and 16 cm. However, at most depths the highest values of DIC and TA were measured at morning LT concurrent with the lowest values of pH_T (Fig. 6).

3.3.2.2 Mangrove Bay, Bermuda Similar to Mission Bay, DIC and TA were strongly coupled. The tidal signal observed in the water column was also seen at 2 and 8 cm depth in the sediment (Fig. 7). At 6 cm, not only were DIC and TA highest and pH_T and Ω_{Ar} lowest, but the values stayed relatively constant throughout the study. At this depth, variability ($\pm 1\sigma$) of DIC and TA between all 10 samplings was only 48 and 45 $\mu\text{mol kg}^{-1}$, respectively, as compared to bottom water where these parameters on average varied ($\pm 1\sigma$) by 212 and 140 $\mu\text{mol kg}^{-1}$ (Table 2, Fig. 6).

3.4 TA:DIC Relationships

For all three sites, linear regressions of TA and DIC in the porewater were strongly correlated with R^2 values close to 1 ($R^2 \geq 0.98$, $p < 0.001$) (Fig. 8). In Mission Bay, TA:DIC slopes ($\pm 95\%$ CI) of the unvegetated (0.89 ± 0.06) and vegetated (0.90 ± 0.01) sites were similar whereas the slope in Mangrove Bay was 0.85 ± 0.03 . In the bottom water, however, the TA:DIC slopes were considerably lower compared to the slopes of the porewater in both Mission Bay (0.56 ± 0.13) and Mangrove Bay (0.65 ± 0.14) (Fig. 8).

Table 2 Mean ($\pm 1\sigma$) dissolved oxygen, dissolved inorganic carbon, total alkalinity, pH and aragonite saturation state at the Mission Bay bottom water ($n=4$), surface water at the offshore reference site ($n=4$) and in the Mangrove Bay bottom water ($n=13$)

Parameter	Mission Bay	Mission Bay (offshore)	Mangrove Bay
DO ($\mu\text{mol kg}^{-1}$)	246 ± 33	242 ± 23	206 ± 47
DIC ($\mu\text{mol kg}^{-1}$)	2084 ± 42	2099 ± 40	2144 ± 212
TA ($\mu\text{mol kg}^{-1}$)	2291 ± 25	2296 ± 25	2425 ± 140
pH _T	7.96 ± 0.05	7.94 ± 0.04	7.78 ± 0.18
Ω_{Ar}	2.40 ± 0.21	2.32 ± 0.16	3.31 ± 0.83

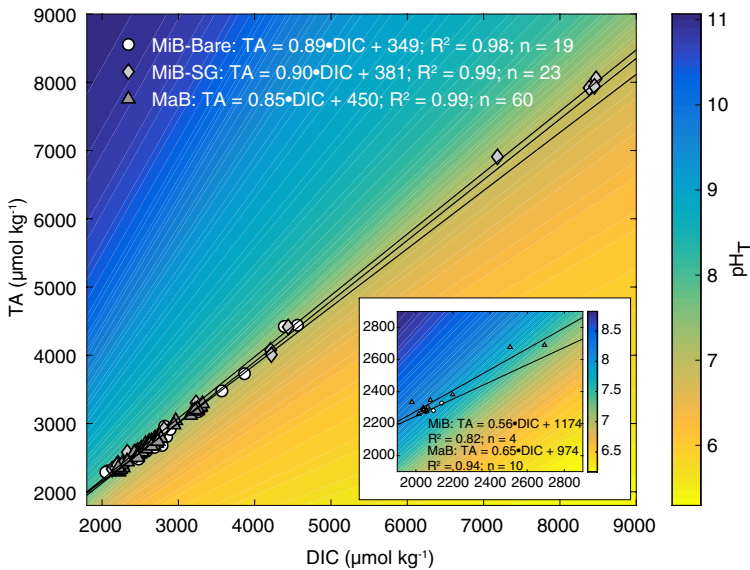
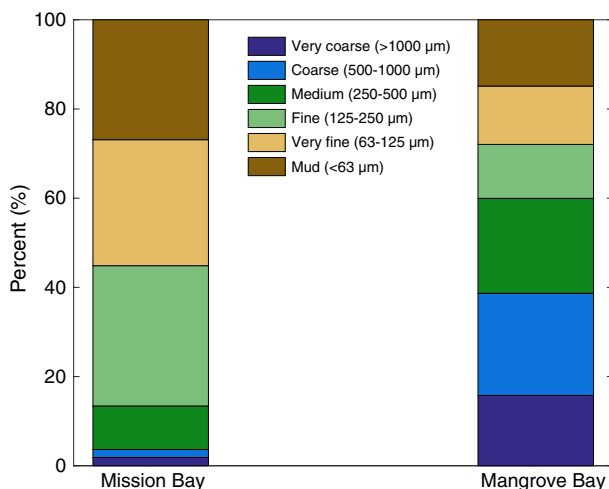


Fig. 8 Property-property plot with model II linear regression showing correlation ($p < 0.001$) between pore-water TA and DIC in Mission Bay Bare (circles), Mission Bay seagrass (diamonds) and Mangrove Bay (triangles). Color isopleths show calculated pH_T. Enfolded plot shows TA:DIC of bottom waters (0 cm) in Mission Bay (filled circles) and Mangrove Bay (filled triangles)

3.5 Sediment Grain Size Distribution

In Mission Bay, grain size distributions were similar between the vegetated (median $\phi = 3.56$) and unvegetated site (median $\phi = 3.48$). The major grain size fractions for both sites were 125–250 μm (Bare: 31%; SG: 31%), <63 μm (Bare: 28%; SG: 26%) and 63–125 μm (Bare: 27%; SG: 29%) (Fig. 9). Sediments in Mangrove Bay (median $\phi = 1.76$) had larger fractions of 500–1000 μm and 1000–2000 μm (mean $\pm 1\sigma$) of $23 \pm 9\%$ and $16 \pm 9\%$, respectively (Fig. 9).

Fig. 9 Grain size distribution in Mission Bay (average of seagrass and bare sites) and Mangrove Bay (average of 5 locations around the PWW site)



4 Discussion

In terms of the main objectives of this study, the results demonstrated that: (i) there was variable connectivity between the water column and the porewater at the different study sites, characterized by different temperature time lags and co-correlation of carbonate chemistry parameters in the porewater and the overlying water column, (ii) there were distinct differences in porewater carbonate chemistry between sites as a function of vegetation, sediment depth and time, and (iii) the diel variability was influenced by a combination of tidal and diurnal light cycles with the Bermuda system being strongly influenced by the semi-diurnal tidal cycles whereas only weak influences were distinguishable for the Mission Bay system. The possible properties responsible for the observed trends and variability are discussed in the subsequent sections.

4.1 Water Column Variability

Although variations in water column temperature over the 24-h study in Mission Bay revealed a distinct tidal signal, it is difficult to infer any clear trend from the other measured parameters due to the coarse temporal sampling resolution (Fig. 4). Yet, the highest values of DIC and TA, and the lowest values of pH_T , Ω_{Ar} and DO, were observed at the two morning samplings and the observed variability over 24 h was likely due to a mixed effect of light intensity and tides (Fig. 4). During the mornings, the water column had experienced a full night of respiration (producing CO_2 and consuming O_2) whereas the afternoon sampling revealed a signal of net primary production (consuming CO_2 and producing O_2) (Cyronak et al. 2018a). Similar lowered DIC and elevated pH_T was observed during the evening sampling, which, coincident with high tide, revealed the influence of open ocean conditions. Further, long-term measurements of temperature showed that variability was influenced both by irradiance and tides, where the temperature increased at low tide and was especially pronounced when it coincided with high irradiance (Online resource 2).

In Mangrove Bay, on the other hand, the influence of the tidal signal was observed in all water column parameters and was much more prevalent than the relatively weak diurnal

signal, which is in agreement with observations by Zablocki et al. (2011) from the same site. The amplitude of DIC and TA between low and high tide was up to 6 times higher compared to Mission Bay (Fig. 4). This is likely due to geomorphological and physical differences between Mangrove and Mission Bay. Mangrove Bay is located in a restricted channel and is much smaller and shallower than Mission Bay, which results in greater tidal flow rates and variability in biogeochemical parameters. Mangrove Bay is also influenced by submarine groundwater discharge (SGD) (Zablocki et al. 2011) and at the same time more directly connected to the open ocean than Mission Bay, leading to large gradients between these end-members. This was evident from the changes in water column parameters during incoming and outgoing tides, where the largest change in between two consecutive samplings occurred between afternoon slack low tide and the following sampling during flood tide. Based on our observations, SGD and tidal pumping owing to rapid tidal flow (Santos et al. 2012) were probably more important factors in Mangrove Bay (Zablocki et al. 2011) than in Mission Bay.

4.2 Spatiotemporal Variability in Porewater Carbonate Parameters

Porewater profiles of carbonate parameters exhibited strong concentration gradients at all sites but differed substantially in both vertical and temporal variability. In Mission Bay, there was a marked difference in the vertical porewater profiles of biogeochemical parameters between the vegetated and unvegetated sites, both in terms of absolute concentrations and vertical variability (Fig. 6). At both sites, DIC and TA increased with sediment depth, but reached almost twice as high concentrations at the deepest depths (12 and 16 cm) in the vegetated compared to the unvegetated sediments (Fig. 6). Over the course of the diel sampling period, this largely contributed to a depth-integrated average of DIC and TA that was 40–50% higher in the vegetated sediments than in the unvegetated. We hypothesize that this difference is due to increased seagrass detritus and labile OM from seagrass root exudates (Blaabjerg et al. 1998; Miyajima et al. 1998; Jones et al. 2003) which fuels microbial remineralization. These DIC and TA profiles observed here resembles those found in seagrass sediments reported by Burdige and Zimmerman (2002) from the Bahamas, where the combined effect of OM supply and oxygen loss from seagrass roots and rhizomes was proposed to induce coupled aerobic remineralization and CaCO_3 dissolution. It is possible that these processes contributed to the difference between vegetated and unvegetated porewater DIC and TA that we observed in Mission Bay.

A general pattern of stable pH_T and Ω_{Ar} at shallow depths followed by a drastic decrease was observed in both vegetated and unvegetated sediments in Mission Bay. However, aragonite undersaturation (i.e., $\Omega_{Ar} < 1$) was shallower in the unvegetated sediments and was common from 6 cm and below. Conversely, aragonite undersaturation was observed at 12 cm in the vegetated sediments, but further work is necessary to assess the underlying mechanisms for this difference between vegetated and unvegetated sediments.

The porewater profiles in Mangrove Bay contrasted to those observed in Mission Bay, both in terms of vertical patterns and temporal variability (Figs. 6, 7). The maximum DIC and TA concentrations were never as high as those in Mission Bay, and depth-integrated average concentrations were about 60% lower than at the Mission Bay seagrass site. At 6 cm depth, DIC and TA reached their maxima with the resulting pH minimum and occasional undersaturation of Ω_{Ar} , but below this depth both pH_T and Ω_{Ar} were generally higher than in Mission Bay (Fig. 6). A similar pattern was observed by Drupp et al. (2016) in bare-substrate CaCO_3 sediment porewater profiles from Hawaii, where a sharp drop in pH

of up to 0.6 units was observed between the SWI and 6 cm, followed by an increase below 8 cm. These vertical trends reflect how different redox processes and subsequent mineral reactions prevail at different depths with aerobic respiration and CaCO_3 dissolution predominant in oxic surface layers (sediment depth < 6 cm in Mangrove Bay and ≤ 8 cm in Mission Bay), and sulfate reduction coupled with either CaCO_3 dissolution or precipitation (depending on the extent of the sulfate reduction reaction) predominant under anoxic conditions at sediment depths > 6 cm in Mangrove Bay and > 8 cm in Mission Bay (e.g., Morse and Mackenzie 1990; Ku et al. 1999; Jahnke and Jahnke 2004; Burdige et al. 2008; Mackenzie and Andersson 2011; Rao et al. 2014; Drupp et al. 2016).

In general, a gradual decrease in the influence of advective transport is expected as a function of sediment depth (Shum 1992; Santos et al. 2012; Drupp et al. 2016), yielding a lower spatial and temporal variability at greater depths. The temporal variability of carbonate parameters in Mangrove Bay largely followed this pattern, with a deviation at 8 cm depth, where variability was higher than at neighboring sediment depths. Notably, at 6 cm depth the variability was lowest and exhibited the highest porewater DIC and TA concentrations (Figs. 6, 7).

In addition to a well-defined tidal signal in the Mangrove Bay porewater, the average time lag of temperature changes between 8 and 16 cm was just under an hour while it was almost three hours in Mission Bay. This is likely due to a combination of increased flushing of seawater and higher sediment permeability in Mangrove Bay relative to Mission Bay. For example, the coarser median grain size and higher fraction of coarse and very coarse sand in Mangrove Bay (Fig. 9) suggest higher sediment permeability in Mangrove Bay than in Mission Bay (but see Bennett et al. 1990). Further, the three times faster temperature changes between 8 and 16 cm (Fig. 5) implies that the Mangrove Bay sediments have higher hydraulic conductivity than in Mission Bay. This difference in porewater residence times between Mission Bay and Mangrove Bay could explain a significant part of the observed difference in DIC and TA, with much higher concentrations at depth in the former site due to diffusion limited transport.

4.3 Methodological Considerations and Future Direction

Porewater systems are characterized by multiple redox conditions and multiple metabolic processes and mineral reactions modify porewater carbonate chemistry [e.g., aerobic oxidation, sulfate reduction, denitrification, CaCO_3 precipitation and dissolution (Krumins et al. 2013)]. Yet, few attempts have been made to fully characterize early diagenesis in seagrass sediments (Eldridge and Morse 2000; Hebert 2005; Hu 2007) and many open-ended questions remain to be resolved including quantifying the relative contribution from different biogeochemical processes to spatiotemporal variability of porewater DIC and TA. Although such a characterization is beyond the present study, a means to discern the *net* contribution from a combination of biogeochemical processes is by linear regression analysis of TA and DIC concentrations (Fig. 1; Deffeyes 1965; Moulin et al. 1985; Mackenzie and Andersson 2011; Drupp et al. 2016; Cyronak et al. 2018b). In the bottom waters at the two study locations, the non-salinity normalized TA:DIC slopes reflect the influences from a combination of these processes and mixing of porewater and the overlying seawater. In contrast, due to the restricted flow in the sediments, the porewater TA:DIC slopes are most strongly controlled by the prevailing porewater biogeochemical processes. This includes differential metabolic modification of DIC and TA dependent on the oxidation state, as well as DIC and TA production and consumption from CaCO_3 dissolution and precipitation

reactions, respectively (Morse and Mackenzie 1990; Burdige 2006). Based on studies from environments similar to Mangrove Bay, the observed slope close to 1 (0.85) in the porewaters was most likely a reflection of metabolically driven CaCO_3 dissolution under aerobic conditions followed by sulfate reduction as the dominant process in the anaerobic parts of the sediments, potentially accompanied by CaCO_3 precipitation (Moulin et al. 1985; Morse and Mackenzie 1990; Andersson et al. 2007; Mackenzie and Andersson 2011; Drupp et al. 2016). In Mission Bay, the high TA and DIC concentrations in combination with qualitative observations of HgS precipitation following HgCl_2 poisoning and strong H_2S odors from porewater samples suggest that net sulfate reduction is a dominant anaerobic redox process (Holmer and Nielsen 1997). CaCO_3 dissolution could also be important at this location, despite lower abundance of CaCO_3 substrates, but further research will be needed to establish the relative influence of CaCO_3 dissolution on porewater chemistry in these siliciclastic sediments.

Bioturbation and bioirrigation strongly affect the transport of solutes and redox conditions in porewaters (Aller 1982; Huettel and Gust 1992; Aller and Aller 1998). Several studies have found higher infaunal abundance in vegetated compared to unvegetated sediments (Stoner 1980; Edgar et al. 1994; Boström and Bonsdorff 1997; Fredriksen et al. 2010), suggesting that these additional infauna may have a greater effect on redox conditions and solute transport in sediments underlying seagrass beds. The role they play in modifying porewater carbonate chemistry within the rhizosphere, particularly in relation to ROL, should be investigated further.

Tides, currents and wave action can all induce a pressure gradient sufficient to drive advective transport in and out of the sediments, carrying solutes (e.g., DIC and TA) present in the porewater (Huettel and Webster 2001). If the sediment is readily flushed (i.e., advective forces dominate) a tidal signal could be represented in the temporal variability of porewater biogeochemistry, such as seen in Mangrove Bay (Ovalle et al. 1990; Jahnke et al. 2005; Zablocki et al. 2011; Drupp et al. 2016). Sediment properties and physical processes therefore need to be well-characterized across space and time in future assessments of porewater biogeochemistry, especially in vegetated sediments where small-scale spatial variability can be significant.

In conclusion, this study highlights the variable nature of porewater biogeochemistry on different spatial and temporal scales and examines the differences between seagrass-dominated sediment compared to unvegetated sediment in two distinctly different locations. These initial observations, utilizing comparable methods across sites, serve as a starting point for future studies aimed at elucidating the underlying mechanisms controlling the vertical and temporal variability in porewater carbonate chemistry in vegetated and unvegetated sediments. Seagrass seems to induce higher accumulation of DIC and TA in the porewaters compared to unvegetated sediments, possibly due to higher OM deposition in conjunction with oxygen loss from the roots, but further investigation is needed to decisively test this hypothesis in different seagrass systems. Future research should also focus on constraining the interaction between physicochemical setting and early diagenetic processes and its effect on spatiotemporal variability of carbonate chemistry. As illustrated here, environmental differences such as tidal regime and sediment characteristics can affect the short-term variability in carbonate chemistry, and changes in the water column can influence the sediment porewater chemistry in variable ways. The demonstrated connectivity between sediment and overlying water column implies that fluxes of DIC and TA between these waters can be significant. Thus, these features need to be considered in biogeochemical models and future assessments of coastal carbon cycling.

Acknowledgements Open access funding provided by Lund University. This study was conducted in part at the Kendall-Frost Mission Bay Marsh Reserve of the University of California National Reserve System (UCNRS). Funding was received from National Science Foundation OCE 12-55042 (AJA). The constructive reviews of David J. Burdige and two anonymous referees are gratefully acknowledged.

Funding Funding was received from National Science Foundation OCE 12-55042 (AJA).

Compliance with Ethical Standards

Conflict of interest The authors declare that they have no conflict of interest.

Open Access This article is licensed under a Creative Commons Attribution 4.0 International License, which permits use, sharing, adaptation, distribution and reproduction in any medium or format, as long as you give appropriate credit to the original author(s) and the source, provide a link to the Creative Commons licence, and indicate if changes were made. The images or other third party material in this article are included in the article's Creative Commons licence, unless indicated otherwise in a credit line to the material. If material is not included in the article's Creative Commons licence and your intended use is not permitted by statutory regulation or exceeds the permitted use, you will need to obtain permission directly from the copyright holder. To view a copy of this licence, visit <http://creativecommons.org/licenses/by/4.0/>.

References

- Aller RC (1982) Carbonate dissolution in nearshore terrigenous muds: the role of physical and biological reworking. *J Geol* 90:79–95. <https://doi.org/10.1086/628652>
- Aller RC, Aller JY (1998) The effect of biogenic irrigation intensity and solute exchange on diagenetic reaction rates in marine sediments. *J Mar Res* 56:905–936. <https://doi.org/10.1357/002224098321667413>
- Andersson AJ, Bates NR, Mackenzie FT (2007) Dissolution of carbonate sediments under rising pCO₂ and ocean acidification: observations from Devil's Hole, Bermuda. *Aquat Geochem* 13:237–264. <https://doi.org/10.1007/s10498-007-9018-8>
- Andersson AJ, Yeakel KL, Bates NR, de Putron SJ (2014) Partial offsets in ocean acidification from changing coral reef biogeochemistry. *Nat Clim Chang* 4:56–61. <https://doi.org/10.1038/nclimate2050>
- Barron C, Duarte CM, Frankignoulle M, Borges AV (2006) Organic carbon metabolism and carbonate dynamics in a Mediterranean seagrass (*Posidonia oceanica*) meadow. *Estuaries Coasts* 29:417–426. <https://doi.org/10.1007/BF02784990>
- Bauer JE, Cai WJ, Raymond PA, Bianchi TS, Hopkinson CS, Regnier PAG (2013) The changing carbon cycle of the coastal ocean. *Nature* 504:61–70. <https://doi.org/10.1038/nature12857>
- Bennett RH et al (1990) In situ porosity and permeability of selected carbonate sediment: Great Bahama Bank Part 1: measurements. *Mar Georesour Geotechnol* 9:1–28. <https://doi.org/10.1080/10641199009388227>
- Blaabjerg V, Mouritsen KN, Finster K (1998) Diel cycles of sulphate reduction rates in sediments of a *Zostera marina* bed (Denmark). *Aquat Microb Ecol* 15:97–102. <https://doi.org/10.3354/ame015097>
- Blott SJ, Pye K (2001) GRADISTAT: a grain size distribution and statistics package for the analysis of unconsolidated sediments. *Earth Surf Process Landf* 26:1237–1248
- Bockmon EE, Dickson AG (2014) A seawater filtration method suitable for total dissolved inorganic carbon and pH analyses. *Limnol Oceanogr*: Methods 12:191–195. <https://doi.org/10.4319/lom.2014.12.191>
- Borum J, Sand-Jensen K, Binzer T, Pedersen O, Greve TM (2007) Oxygen movement in seagrasses. In: Larkum AWD, Orth RJ, Duarte CM (eds) *Seagrasses: biology, ecology and conservation*. Springer, Dordrecht, pp 255–270. <https://doi.org/10.1007/978-1-4020-2983-7>
- Boström C, Bonsdorff E (1997) Community structure and spatial variation of benthic invertebrates associated with *Zostera marina* (L.) beds in the northern Baltic Sea. *J Sea Res* 37:153–166. [https://doi.org/10.1016/S1385-1101\(96\)00007-X](https://doi.org/10.1016/S1385-1101(96)00007-X)
- Bouillon S et al (2007) Importance of intertidal sediment processes and porewater exchange on the water column biogeochemistry in a pristine mangrove creek (Ras Dege, Tanzania). *Biogeosci Discuss* 4:317–348

- Brodersen KE, Koren K, Lichtenberg M, Kühl M (2016) Nanoparticle-based measurements of pH and O₂ dynamics in the rhizosphere of *Zostera marina* L.: effects of temperature elevation and light-dark transitions. *Plant, Cell Environ* 39:1619–1630. <https://doi.org/10.1111/pce.12740>
- Brodersen KE, Siboni N, Nielsen D, Pernice M, Ralph P, Seymour J, Kühl M (2018) Seagrass rhizosphere microenvironment alters plant-associated microbial community composition. *Environ Microbiol*. <https://doi.org/10.1111/1462-2920.14245>
- Burdige DJ (2006) *Geochemistry of marine sediments*. Princeton University Press, Princeton
- Burdige DJ, Zimmerman RC (2002) Impact of sea grass density on carbonate dissolution in Bahamian sediments. *Limnol Oceanogr* 47:1751–1763. <https://doi.org/10.4319/lo.2002.47.6.1751>
- Burdige DJ, Zimmerman RC, Hu X (2008) Rates of carbonate dissolution in permeable sediments estimated from pore-water profiles: the role of sea grasses. *Limnol Oceanogr* 53:549–565. <https://doi.org/10.4319/lo.2008.53.2.0549>
- Caffrey J, Kemp W (1991) Seasonal and spatial patterns of oxygen production, respiration and root-rhizome release in *Potamogeton perfoliatus* L. and *Zostera marina* L. *Aquat Bot* 40:109–128. [https://doi.org/10.1016/0304-3770\(91\)90090-R](https://doi.org/10.1016/0304-3770(91)90090-R)
- Camp EF, Suggett DJ, Gendron G, Jompa J, Manfrino C, Smith DJ (2016) Mangrove and seagrass beds provide different biogeochemical services for corals threatened by climate change. *Front Mar Sci*. <https://doi.org/10.3389/fmars.2016.00052>
- Cyronak T et al (2018a) Short-term spatial and temporal carbonate chemistry variability in two contrasting seagrass meadows: implications for pH buffering capacities. *Estuaries Coasts*. <https://doi.org/10.1007/s12237-017-0356-5>
- Cyronak T et al (2018b) Taking the metabolic pulse of the world's coral reefs. *PLoS ONE* 13:e0190872. <https://doi.org/10.1371/journal.pone.0190872>
- Deborde J et al (2008) Role of tidal pumping on nutrient cycling in a temperate lagoon (Arcachon Bay, France). *Mar Chem* 109:98–114. <https://doi.org/10.1016/j.marchem.2007.12.007>
- Deffeyes KS (1965) Carbonate equilibria: a graphic and algebraic approach. *Limnol Oceanogr* 10:412–426. <https://doi.org/10.4319/lo.1965.10.3.0412>
- Delgard ML et al (2016) Biogeochemistry of dissolved inorganic carbon and nutrients in seagrass (*Zostera noltei*) sediments at high and low biomass. *Estuar Coast Shelf Sci* 179:12–22. <https://doi.org/10.1016/j.ecss.2016.01.012>
- DeValls T, Dickson A (1998) The pH of buffers based on 2-amino-2-hydroxymethyl-1, 3-propanediol ('tris') in synthetic sea water. *Deep Sea Res Part I* 45:1541–1554. [https://doi.org/10.1016/S0967-0637\(98\)00019-3](https://doi.org/10.1016/S0967-0637(98)00019-3)
- Dickson AG, Goyet C (1994) *Handbook of methods for the analysis of the various parameters of the carbon dioxide system in sea water, version 2*. Oak Ridge National Lab., TN, USA
- Dickson AG, Sabine CL, Christian JRE (2007) Guide to best practices for ocean CO₂ measurements. *PICES Special Publ* 3:191
- Drupp PS, De Carlo EH, Mackenzie FT (2016) Porewater CO₂–carbonic acid system chemistry in permeable carbonate reef sands. *Mar Chem* 185:48–64. <https://doi.org/10.1016/j.marchem.2016.04.004>
- Duarte CM, Middelburg JJ, Caraco N (2005) Major role of marine vegetation on the oceanic carbon cycle. *Biogeosciences* 2:1–8. <https://doi.org/10.5194/bg-2-1-2005>
- Edgar G, Shaw C, Watson G, Hammond L (1994) Comparisons of species richness, size-structure and production of benthos in vegetated and unvegetated habitats in Western Port, Victoria. *J Exp Mar Biol Ecol* 176:201–226. [https://doi.org/10.1016/0022-0981\(94\)90185-6](https://doi.org/10.1016/0022-0981(94)90185-6)
- Eldridge PM, Morse JW (2000) A diagenetic model for sediment–seagrass interactions. *Mar Chem* 70:89–103. [https://doi.org/10.1016/S0304-4203\(00\)00018-9](https://doi.org/10.1016/S0304-4203(00)00018-9)
- Elliott DT, Kaufmann RS (2007) Spatial and temporal variability of mesozooplankton and tintinnid ciliates in a seasonally hypersaline estuary. *Estuaries Coasts* 30:418–430. <https://doi.org/10.1007/BF02819388>
- Falter JL, Sansone FJ (2000) Shallow pore water sampling in reef sediments. *Coral Reefs* 19:93–97. <https://doi.org/10.1007/s003380050233>
- Fourqurean JW et al (2012) Seagrass ecosystems as a globally significant carbon stock. *Nat Geosci* 5:505–509. <https://doi.org/10.1038/ngeo1477>
- Frederiksen MS, Glud RN (2006) Oxygen dynamics in the rhizosphere of *Zostera marina*: a two-dimensional planar optode study. *Limnol Oceanogr* 51:1072–1083. <https://doi.org/10.4319/lo.2006.51.2.1072>
- Fredriksen S, De Backer A, Boström C, Christie H (2010) Infauna from *Zostera marina* L. meadows in Norway. Differences in vegetated and unvegetated areas. *Mar Biol Res* 6:189–200. <https://doi.org/10.1080/17451000903042461>
- Goyet C, Bradshaw AL, Brewer PG (1991) The carbonate system in the Black sea. *Deep-Sea Res Part a-Oceanogr Res Pap* 38:S1049–S1068. [https://doi.org/10.1016/S0198-0149\(10\)80023-8](https://doi.org/10.1016/S0198-0149(10)80023-8)


- Gran G (1952) Determination of the equivalence point in potentiometric titrations. Part II. *Analyst* 77:661–671
- Greve TM, Borum J, Pedersen O (2003) Meristematic oxygen variability in eelgrass (*Zostera marina*). *Limnol Oceanogr* 48:210–216. <https://doi.org/10.4319/lo.2003.48.1.0210>
- Hebert AB (2005) Diagenesis in seagrass vegetated sediments: biogeochemical processes on diurnal time scales. Ph.D. thesis, Texas A&M University
- Hendriks IE et al (2014) Photosynthetic activity buffers ocean acidification in seagrass meadows. *Biogeosciences* 11:333–346. <https://doi.org/10.5194/bg-11-333-2014>
- Hines ME, Lyons WB (1982) Biogeochemistry of nearshore Bermuda sediments. I. Sulfate reduction rates and nutrient generation. *Mar Ecol-Prog Ser*, 87–94
- Holmer M, Nielsen SL (1997) Sediment sulfur dynamics related to biomass-density patterns in *Zostera marina* (eelgrass) beds. *Mar Ecol-Prog Ser* 146:163–171
- Howard J et al (2017) Clarifying the role of coastal and marine systems in climate mitigation. *Front Ecol Environ* 15:42–50. <https://doi.org/10.1002/fee.1451>
- Hu X (2007) Seagrass-mediated carbonate dissolution and early diagenesis in Bahamas Bank sediments. Ph.D. thesis, Old Dominion University
- Huettel M, Gust G (1992) Solute release mechanisms from confined sediment cores in stirred benthic chambers and flume flows. *Mar Ecol-Prog Ser*, 187–197
- Huettel M, Webster IT (2001) Porewater flow in permeable sediments. In: Boudreau BP, Jørgensen BB (eds) *The benthic boundary layer: transport processes and biogeochemistry*. Oxford University Press, New York, pp 144–179
- Ingemann Jensen S, Kühl M, Glud RN, Jørgensen LB, Priemé A (2005) Oxidic microzones and radial oxygen loss from roots of *Zostera marina*. *Mar Ecol-Prog Ser Online* 293:49–58
- Invers O, Zimmerman RC, Alberte RS, Pérez M, Romero J (2001) Inorganic carbon sources for seagrass photosynthesis: an experimental evaluation of bicarbonate use in species inhabiting temperate waters. *J Exp Mar Biol Ecol* 265:203–217. [https://doi.org/10.1016/S0022-0981\(01\)00332-X](https://doi.org/10.1016/S0022-0981(01)00332-X)
- Jahnke RA, Jahnke DB (2004) Calcium carbonate dissolution in deep sea sediments: reconciling microelectrode, pore water and benthic flux chamber results. *Geochim Cosmochim Acta* 68:47–59. [https://doi.org/10.1016/S0016-7037\(03\)00260-6](https://doi.org/10.1016/S0016-7037(03)00260-6)
- Jahnke R, Richards M, Nelson J, Robertson C, Rao A, Jahnke D (2005) Organic matter remineralization and porewater exchange rates in permeable South Atlantic Bight continental shelf sediments. *Cont Shelf Res* 25:1433–1452. <https://doi.org/10.1016/j.csr.2005.04.002>
- Johnson MR, Williams SL, Lieberman CH, Solbak A (2003) Changes in the abundance of the seagrasses *Zostera marina* L. (eelgrass) and *Ruppia maritima* L. (widgeongrass) in San Diego, California, following an El Niño event. *Estuaries* 26:106–115. <https://doi.org/10.1007/bf02691698>
- Jones WB, Cifuentes LA, Kaldy JE (2003) Stable carbon isotope evidence for coupling between sedimentary bacteria and seagrasses in a sub-tropical lagoon. *Mar Ecol-Prog Ser* 255:15–25. <https://doi.org/10.3354/meps255015>
- Jourabchi P, Van Cappellen P, Regnier P (2005) Quantitative interpretation of pH distributions in aquatic sediments: a reaction-transport modeling approach. *Am J Sci* 305:919–956
- Knap A et al (1997) BATS Methods manual, version 4. JGOFS Planning Office, Woods Hole
- Krumins V, Gehlen M, Arndt S, Van Cappellen P, Regnier P (2013) Dissolved inorganic carbon and alkalinity fluxes from coastal marine sediments: model estimates for different shelf environments and sensitivity to global change. *Biogeosciences* 10:371–398. <https://doi.org/10.5194/bg-10-371-2013>
- Ku T, Walter L, Coleman M, Blake R, Martini A (1999) Coupling between sulfur recycling and syndepositional carbonate dissolution: evidence from oxygen and sulfur isotope composition of pore water sulfate, South Florida Platform, USA. *Geochim Cosmochim Acta* 63:2529–2546
- Largier J, Hollibaugh JT, Smith S (1997) Seasonally hypersaline estuaries in Mediterranean-climate regions. *Estuar Coast Shelf Sci* 45:789–797. <https://doi.org/10.1006/ecss.1997.0279>
- Lee K-S, Dunton KH (2000) Diurnal changes in pore water sulfide concentrations in the seagrass *Thalassia testudinum* beds: the effects of seagrasses on sulfide dynamics. *J Exp Mar Biol Ecol* 255:201–214. [https://doi.org/10.1016/S0022-0981\(00\)00300-2](https://doi.org/10.1016/S0022-0981(00)00300-2)
- Lessin G et al (2018) Modelling marine sediment biogeochemistry: current knowledge gaps, challenges and some methodological advice for advancement. *Front Mar Sci* 5:19. <https://doi.org/10.3389/fmars.2018.00019>
- Levin LA (1984) Life history and dispersal patterns in a dense infaunal polychaete assemblage: community structure and response to disturbance. *Ecology* 65:1185–1200
- Lewis E, Wallace D (1998) Program developed for CO₂ system calculations. Carbon Dioxide Information Analysis Center, managed by Lockheed Martin Energy Research Corporation for the US Department of Energy Tennessee

- Long MH, Rheuban JE, Berg P, Ziemann JC (2012) A comparison and correction of light intensity loggers to photosynthetically active radiation sensors. *Limnol Oceanogr: Methods* 10:416–424. <https://doi.org/10.4319/lom.2012.10.416>
- Lueker TJ, Dickson AG, Keeling CD (2000) Ocean pCO₂ calculated from dissolved inorganic carbon, alkalinity, and equations for K₁ and K₂: validation based on laboratory measurements of CO₂ in gas and seawater at equilibrium. *Mar Chem* 70:105–119. [https://doi.org/10.1016/S0304-4203\(00\)00022-0](https://doi.org/10.1016/S0304-4203(00)00022-0)
- Lyons W, Wilson K, Armstrong P, Smith G, Gaudette H (1980) Trace-metal pore water geochemistry of nearshore bermuda carbonate sediments. *Oceanol Acta* 3:363–367
- Mackenzie FT, Andersson AJ (2011) Biological control on diagenesis: influence of bacteria and relevance to ocean acidification. In: Reitner J, Thiel V (eds) *Encyclopedia of geobiology*. Springer, Dordrecht, pp 137–143. https://doi.org/10.1007/978-1-4020-9212-1_73
- Mazarrasa I et al (2015) Seagrass meadows as a globally significant carbonate reservoir. *Biogeosciences* 12:4993–5003. <https://doi.org/10.5194/bg-12-4993-2015>
- Menne MJ, Durre I, Vose RS, Gleason BE, Houston TG (2012) An overview of the global historical climatology network-daily database. *J Atmos Ocean Technol* 29:897–910. <https://doi.org/10.1175/JTECH-D-11-00103.1>
- Middelburg JJ (2018) Reviews and syntheses: to the bottom of carbon processing at the seafloor. *Biogeosciences* 15:413–427. <https://doi.org/10.5194/bg-15-413-2018>
- Migné A, Davoult D, Spilmont N, Ouisse V, Boucher G (2016) Spatial and temporal variability of CO₂ fluxes at the sediment–air interface in a tidal flat of a temperate lagoon (Arcachon Bay, France). *J Sea Res* 109:13–19. <https://doi.org/10.1016/j.seares.2016.01.003>
- Miyajima T, Koike I, Yamano H, Iizumi H (1998) Accumulation and transport of seagrass-derived organic matter in reef flat sediment of Green Island, Great Barrier Reef. *Mar Ecol-Prog Ser* 175:251–259
- Morse JW, Mackenzie FT (1990) *Geochemistry of sedimentary carbonates*, vol 48. Elsevier, Amsterdam
- Moulin E, Jordens A, Wollast R (1985) Influence of the aerobic bacterial respiration on the early dissolution of carbonates in coastal sediments. In: *Proceedings progress in Belgium Oceanographic Research*, Brussels
- Mucci A, Sundby B, Gehlen M, Arakaki T, Zhong S, Silverberg N (2000) The fate of carbon in continental shelf sediments of eastern Canada: a case study. *Deep Sea Res Part II* 47:733–760
- Nellemann C, Corcoran E, Duarte C, Valdés L, De Young C, Fonseca L, Grimsditch G (2009) Blue Carbon: a rapid response assessment. United Nations Environment Programme, GRID-Arendal 80
- Obaza A, Hoffman R, Clausing R (2015) Long-term stability of eelgrass fish assemblages in two highly developed coastal estuaries. *Fisheries Manag Ecol* 22:224–238. <https://doi.org/10.1111/fme.12119>
- Ovalle A, Rezende C, Lacerda L, Silva C (1990) Factors affecting the hydrochemistry of a mangrove tidal creek, Sepetiba Bay, Brazil. *Estuar Coast Shelf Sci* 31:639–650. [https://doi.org/10.1016/0272-7714\(90\)90017-L](https://doi.org/10.1016/0272-7714(90)90017-L)
- Pacella SR, Brown CA, Waldbusser GG, Labiosa RG, Hales B (2018) Seagrass habitat metabolism increases short-term extremes and long-term offset of CO₂ under future ocean acidification. *Proc Natl Acad Sci* 115:3870–3875. <https://doi.org/10.1073/pnas.1703445115>
- Rao AMF, Malkin SY, Montserrat F, Meysman FJR (2014) Alkalinity production in intertidal sands intensified by lugworm bioirrigation. *Estuar Coast Shelf Sci* 148:36–47. <https://doi.org/10.1016/j.ecss.2014.06.006>
- Rassmann J, Lansard B, Pozzato L, Rabouille C (2016) Carbonate chemistry in sediment porewaters of the Rhône River delta driven by early diagenesis (northwestern Mediterranean). *Biogeosciences* 13:5379. <https://doi.org/10.5194/bg-13-5379-2016>
- Rassmann J et al (2018) Impact of ocean acidification on the biogeochemistry and meiofaunal assemblage of carbonate-rich sediments: results from core incubations (Bay of Villefranche, NW Mediterranean Sea). *Mar Chem* 203:102–119. <https://doi.org/10.1016/j.marchem.2018.05.006>
- Sand-Jensen K, Prahm C, Stokholm H (1982) Oxygen release from roots of submerged aquatic macrophytes. *Oikos*, 349–354
- Santos IR, Eyre BD, Huettel M (2012) The driving forces of porewater and groundwater flow in permeable coastal sediments: a review. *Estuar Coast Shelf Sci* 98:1–15. <https://doi.org/10.1016/j.ecss.2011.10.024>
- Semesi IS, Beer S, Björk M (2009) Seagrass photosynthesis controls rates of calcification and photosynthesis of calcareous macroalgae in a tropical seagrass meadow. *Mar Ecol-Prog Ser* 382:41–47. <https://doi.org/10.3354/meps07973>
- Shum K (1992) Wave-induced advective transport below a rippled water-sediment interface. *J Geophys Res: Oceans* 97:789–808. <https://doi.org/10.1029/91JC02101>

- Sippo JZ, Maher DT, Tait DR, Holloway C, Santos IR (2016) Are mangroves drivers or buffers of coastal acidification? Insights from alkalinity and dissolved inorganic carbon export estimates across a latitudinal transect. *Global Biogeochem Cycles* 30:753–766. <https://doi.org/10.1002/2015gb005324>
- Smith RD, Dennison WC, Alberte RS (1984) Role of seagrass photosynthesis in root aerobic processes. *Plant Physiol* 74:1055–1058. <https://doi.org/10.1104/pp.74.4.1055>
- Stoner AW (1980) The role of seagrass biomass in the organization of benthic macrofaunal assemblages. *Bull Mar Sci* 30:537–551
- Taillardat P et al (2018) Carbon dynamics and inconstant porewater input in a mangrove tidal creek over contrasting seasons and tidal amplitudes. *Geochim Cosmochim Acta* 237:32–48. <https://doi.org/10.1016/j.gca.2018.06.012>
- Tait DR, Maher DT, Macklin PA, Santos IR (2016) Mangrove pore water exchange across a latitudinal gradient. *Geophys Res Lett* 43:3334–3341. <https://doi.org/10.1002/2016GL068289>
- Talley DM, Talley TS, Blanco A (2015) Insights into the establishment of the Manila clam on a tidal flat at the southern end of an introduced range in Southern California, USA. *PLoS ONE* 10:13. <https://doi.org/10.1371/journal.pone.0118891>
- Unsworth RKF, Collier CJ, Henderson GM, McKenzie LJ (2012) Tropical seagrass meadows modify seawater carbon chemistry: implications for coral reefs impacted by ocean acidification. *Environ Res Lett* 7:024026. <https://doi.org/10.1088/1748-9326/7/2/024026>
- Winkel A, Borum J (2009) Use of sediment CO₂ by submersed rooted plants. *Ann Bot* 103:1015–1023. <https://doi.org/10.1093/aob/mcp036>
- Zablocki JA, Andersson AJ, Bates NR (2011) Diel aquatic CO₂ system dynamics of a Bermudian mangrove environment. *Aquat Geochem* 17:841. <https://doi.org/10.1007/s10498-011-9142-3>
- Zeebe RE, Wolf-Gladrow DA (2001) CO₂ in seawater: equilibrium, kinetics, isotopes vol. 65. Gulf Professional Publishing

Publisher's Note Springer Nature remains neutral with regard to jurisdictional claims in published maps and institutional affiliations.

Affiliations

Theodor Kindeberg^{1,2,3}  · Nicholas R. Bates^{4,5} · Travis A. Courtney¹ · Tyler Cyronak^{1,7} · Alyssa Griffin¹ · Fred T. Mackenzie⁶ · May-Linn Paulsen¹ · Andreas J. Andersson¹

¹ Scripps Institution of Oceanography, University of California San Diego, 9500 Gilman Drive, La Jolla, CA 92093-0244, USA

² Centre for Environmental and Climate Research, Lund University, Sölvegatan 37, 223 62 Lund, Sweden

³ Present Address: Department of Biology, Lund University, Sölvegatan 37, 223 62 Lund, Sweden

⁴ Bermuda Institute of Ocean Sciences, 17 Biological Station, St. George's GE01, Bermuda

⁵ Ocean and Earth Science, National Oceanography Centre Southampton, University of Southampton, Southampton SO14 3ZH, UK

⁶ Department of Oceanography, University of Hawaii, 1000 Pope Rd., Honolulu, HI 96822, USA

⁷ Department of Marine and Environmental Sciences, Halmos College of Natural Sciences and Oceanography, Nova Southeastern University, 8000 North Ocean Drive, Dania Beach, FL 33004, USA